Journal of Brilliant Engineering 4 (2026) 41165
Brilliant Engineering
journal home: www.acapublishing.com/journals/4/ben

Research Article

Effect of Surfactants on The Structural, Morphological and Thermal Properties of Nickel Borate Synthesized by Co-Precipitation

Eda Keleş Güner,[1], Abdulkadir Özer*,[2]
[1]*Erzincan University, Department of Civil Defense and Firefighting, Üzümlü Vocational School, Erzincan, Turkey*
[2]*Atatürk University, Engineering Faculty, Department of Chemical Engineering, Erzurum, Turkey*

Keywords

Nickel borate,
CTAB,
SB12,
SDS,
Crystal growth,
Morphology control.

Abstract

Nickel borate ($Ni_3(BO_3)_2$) has attracted considerable attention due to its promising applications in catalysis, electrochemical energy storage, magnetic materials, and ceramic technologies. Nickel borate was synthesized via a co-precipitation method using nickel chloride hexahydrate, boric acid as precursor materials, and Cetyltrimethylammonium bromide (CTAB), N-dodecyl-N, N-dimethyl-3-ammoniopropanesulfonate (SB12), Sodium dodecyl sulfate (SDS) as surfactants. The precipitated product was calcined at 800°C to obtain crystalline nickel borate. The synthesized material was characterized using XRD and SEM. TGA analysis confirmed the formation of crystalline nickel borate, while FTIR spectra verified the presence of borate groups. The XRD analysis confirmed the formation of orthorhombic $Ni_3(BO_3)_2$ after calcination at 800°C. SEM observations revealed that SB12 promoted larger spherical crystallites whereas SDS produced finer particles with severe agglomeration. FTIR results show that the type of surfactant affects the binding environment and surface chemistry of the synthesized nickel borate materials, while common B–O related bands confirm that the basic borate structure is preserved in all three samples. These FTIR observations are also consistent with the expected surfactant-dependent differences in morphology and crystal structure observed by SEM and XRD. TG-DTA analysis indicated crystallization around 700°C and demonstrated the highest thermal stability for the CTAB-derived sample. The properties of nickel borate are strongly influenced particularly by the use of surfactant during particle formation. The findings suggest that appropriate surfactant selection can significantly enhance the structural and functional properties of nickel borate materials.

1. Introduction

Metal borates have been used in many industrial fields in recent years due to their potential applications in electronic ceramics, wide bandgap semiconductors, anti-wear additives, catalysts, plastics, and as reinforcements in optical and laser devices [1-4]. Among them, nickel borate is an important transition-metal borate exhibiting excellent thermal stability, corrosion resistance, magnetic properties, and catalytic activity. Nickel borate materials have been investigated for applications in: electrocatalysis, supercapacitors, battery electrodes, gas sensors, magnetic materials, and photocatalysis [5-9]. The properties of nickel borate strongly depend on its crystal structure, particle size, morphology, and synthesis conditions. Various synthesis methods have been employed to produce nickel borate, including co-precipitation, hydrothermal synthesis, solution combustion method, sol-gel processing, and microwave-assisted techniques [10-14].

Nickel orthoborate has been found to crystallize in an orthorhombic cell octahedral structure. Orthoborates have discrete triangular BO3 polyhedrons in their lattices. Nickel borates have two types of Ni atoms, both octahedrally coordinated and linked by O sharing to form a three-dimensional network. As shown in Figure 1, each O atom is surrounded by three Ni atoms and one B atom arranged in a disordered tetrahedron [15].

Among the factors affecting the synthesis process, surfactants play a critical role in tailoring the microstructure of the resulting material. Surfactants are amphiphilic molecules containing both hydrophilic and hydrophobic groups. During synthesis, they adsorb onto specific crystal planes, alter surface energies, and influence particle growth kinetics. Consequently, surfactants can be utilized as structure-directing agents to obtain nickel borate materials with controlled morphology and improved properties. CTAB, a cationic surfactant, contains positively charged fourth-order ammonium groups that can strongly interact with negatively charged species. These interactions generally lead to sharper diffraction peaks and improved crystallinity by facilitating directional crystal growth and enabling the formation of highly crystalline structures. SDS, on the other hand, is an anionic surfactant containing negatively charged sulfate groups. Unlike CTAB, it delays crystal growth by forming transient surface complexes around metal-containing nuclei through electrostatic interactions between molecules and ions, generally resulting in smaller particles and less aggregation. This is due to the improved dispersion of increased electrostatic repulsion between particles and the contribution to a higher specific surface area. SB12 is a zwitterionic surfactant because it contains both positive and negative functional groups within the same molecule. The literature indicates that SB12 provides stable interactions with both ions and species, minimizing aggregation while leading to homogeneous nucleation and controlled particle growth. [16-19]. Although numerous studies have reported the synthesis of nickel borate using hydrothermal, sol-gel and combustion methods, systematic investigations comparing cationic, anionic and zwitterionic surfactants under identical synthesis conditions remain very limited. Therefore, this study aims to clarify how surfactant chemistry influences crystal growth, morphology and thermal stability.

*Corresponding Author: abdulkadirozer04@gmail.com
Received 13 Jul 2026; Revised 14 Aug 2026; Accepted 14 Aug 2026
https://doi.org/10.36937/ben.2026.41165

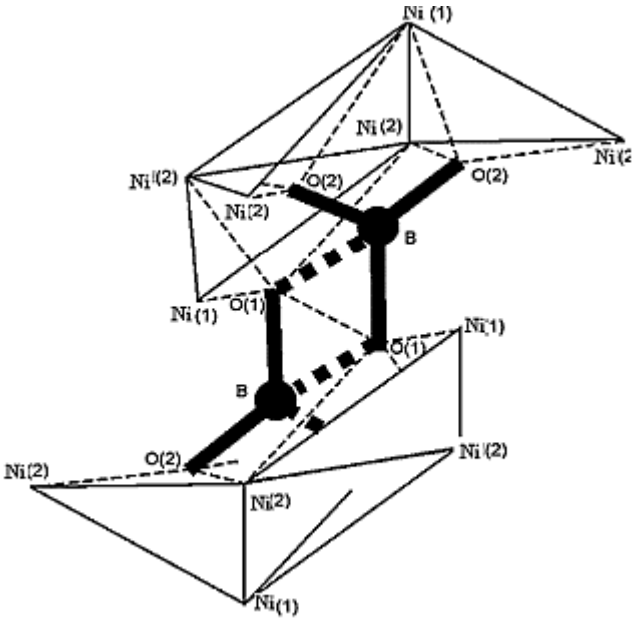

Figure 1. Structure of nickel orthoborate $Ni_3(BO_3)_2$ [15]

2. Experimental Methods

2.1. Materials

The following reagents were used: Nickel chloride hexahydrate ($NiCl_2 \cdot 6H_2O$), Boric acid (H_3BO_3), Sodium hydroxide (NaOH), Cetyltrimethylammonium bromide (CTAB), N-dodecyl-N, N-dimethyl-3-ammoniopropanesulfonate (SB12), Sodium dodecyl sulfate (SDS) and deionized water. All chemicals were of analytical grade and used without further purification.

2.2. Synthesis of Nickel Borate

Nickel borate was prepared by the coprecipitation method. In the synthesis of nickel borate, 0.1 M boric acid solution and 0.003 M surfactant (CTAB, SB12, SDS) were added to a 250 mL reactor and stirred at 750 rpm for 4 h. Then, 0.5 M nickel chloride was added dropwise to the reactant under continuous magnetic stirring, and the reaction was allowed to complete at room temperature for 12 hours. The (Ni:B) ratio was taken as 3:2. The experiments were conducted at pH 8. After the precipitate was filtered, it was washed several times with distilled water and ethanol, and then dried at 100°C for 48 hours. The dried samples were calcined at 800°C for 4 h in air. The obtained powder was stored for further characterization.

2.3. Characterization techniques

The crystal structure and phase composition of the synthesized nickel borate samples were characterized by X-ray diffraction (XRD) using Cu Kα radiation on a PANalytical Empyrean diffractometer. X-ray diffraction measurements were performed using Cu Kα radiation (λ = 1.5406 Å) over a 2θ range of 10–80°. The surface morphology and microstructural characteristics of the nickel borate samples were examined by scanning electron microscopy (SEM) (Zeiss Sigma 300). FTIR measurement was carried out by using a Perkin Elmer Instrument in the wave number range of 400–4000 cm-1. Thermogravimetric analysis of the nickel borate sample was performed on an NETZSCH STA 409 PC Luxx. The calcined a-Al2O3 powder was used as the standard reference.

3. Result and Discussion

3.1. XRD Analysis

The X-ray diffraction (XRD) patterns of the synthesized nickel borate samples are presented in Figure 2. The XRD results of the nickel borate sample synthesized at room temperature show that it has an amorphous structure (Figure 2a). Figure 2(b) presents the X-ray diffraction (XRD) patterns of nickel borate samples synthesized using CTAB, SB12, and SDS surfactants followed by calcination at 800 °C.

All diffraction patterns exhibit well-defined and sharp diffraction peaks, indicating the formation of highly crystalline nickel borate in all samples. The diffraction peaks observed at approximately 2θ = 22–70° can be indexed to the (001), (101), (111), (121), (130), (211), (131), (141), (202), (132), (321), (330), (232), (060), and (251) crystallographic planes. All the diffraction peaks in the XRD pattern can be indexed to orthorhombic $Ni_3(BO_3)_2$ (JCPDS card 75-1809). The presence of identical diffraction peaks for all three samples suggests that the use of different surfactants does not alter the crystal phase of nickel borate but mainly affects its crystallization behavior. (121) plane has the highest diffraction intensity, which is evidence that crystal growth occurs in the crystallographic direction. The absence of peaks corresponding to impurity compounds indicates that the synthesized nickel borate samples have high phase purity. Although the crystal structure remained the same, differences were detected in the peak intensities and widths of the samples synthesized with all three surfactants. The sample synthesized with SDS surfactant has sharper and more intense diffraction peaks compared to CTAB and SB12. Rather than altering the crystal structure of the surfactant, it appears to primarily affect the nucleation and crystal growth processes during synthesis.

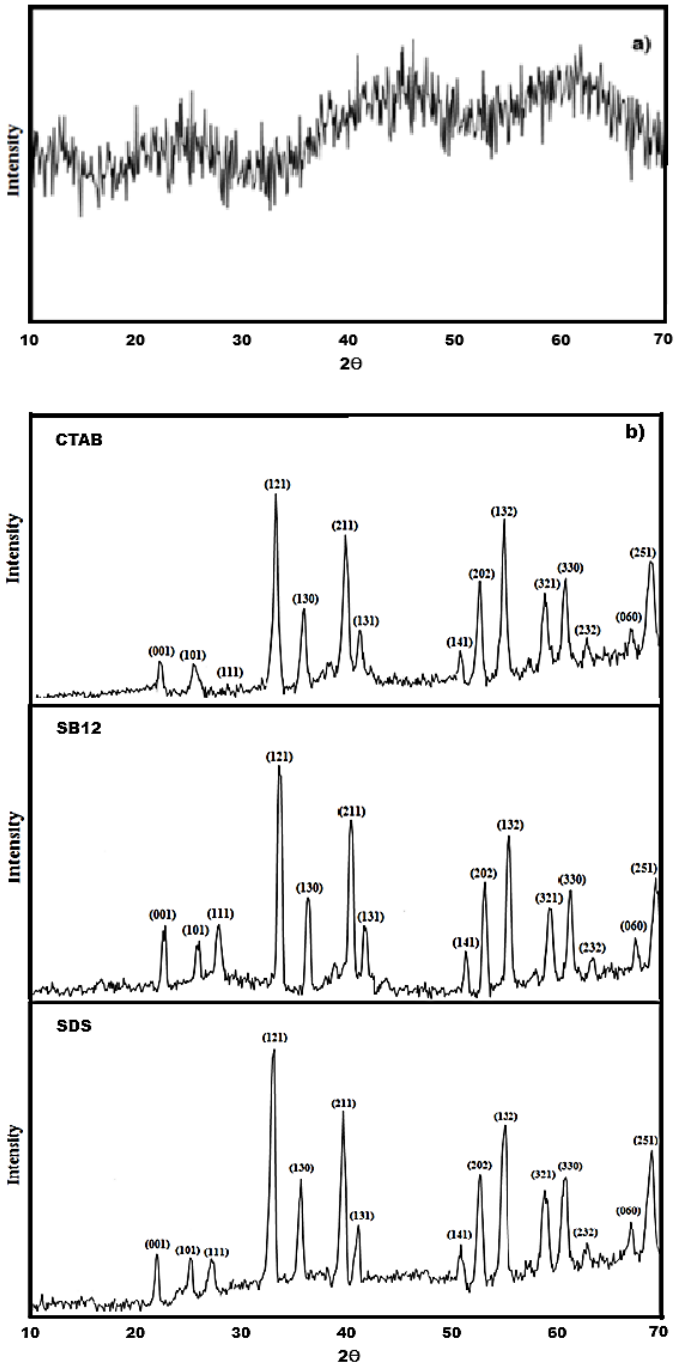

Figure 2. XRD spectra of nickel borate samples (a) room temperature, (b) synthesized in CTA, SB12, and SDS surfactants and calcined at 800°C

3.2. SEM Analysis

SEM micrographs of nickel borate samples synthesized using different surfactants such as CTAB, SB12, and SDS are given in Figure 3. The micrographs show that the type of surfactant has a significant effect on the morphological structure of the synthesized samples.

The nickel borate samples synthesized with CTAB surfactant consists of fine nanoparticles and has a homogeneous morphology, as seen in Figure 3a. This homogeneous morphology indicates that CTAB surfactant effectively controls the nucleation of nanoparticles during synthesis. As shown in Figure 3b, the formation of spherical particles with a cauliflower-like structure was detected in nickel borate samples synthesized with SB12. A porous structure consisting of interparticle spaces is observed in the SB12 sample. In nickel borate samples synthesized with SDS, the formation of largely clustered fine nanoparticles is observed in Figure 3c. It is observed that the nanoparticles obtained from SDS samples are smaller than those obtained from the SB12 sample. The results obtained from SEM images show that the surfactants significantly alter the microstructure of nickel borate, and it is predicted that these morphological differences may also affect the surface area, crystallinity, and catalytic performance of nickel borate.

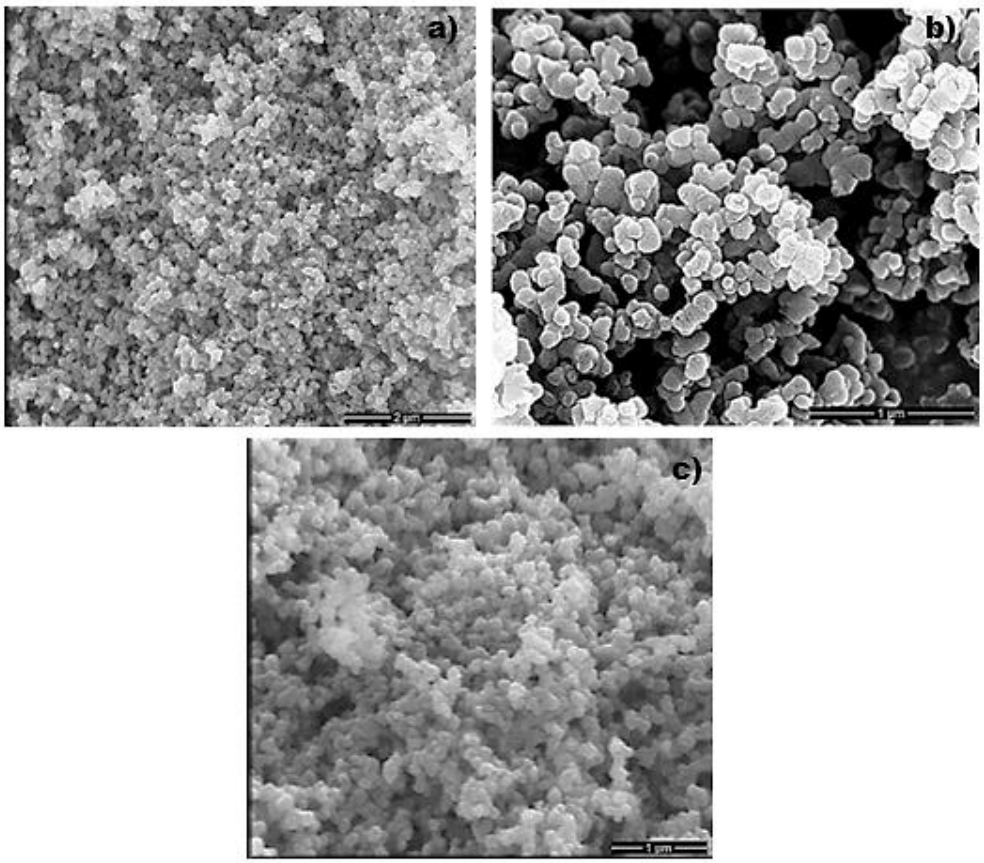

Figure 3. SEM image of nickel borate samples synthesized in a) CTAB, b) SB12, and c) SDS surfactants

3.3. FTIR Analysis

The FTIR spectra of nickel borate samples synthesized in the presence of CTAB, SB12, and SDS surfactants are given in Figure 4.

Characteristic low-wavelength absorption bands in the 600–1500 cm^{-1} region are observed in all three samples, and these bands indicate the vibrational modes of the borate skeleton. Bands observed around 573–695 cm^{-1} are associated with B–O–B bending and metal-oxygen vibrations that enable the formation of nickel-borate phases. The differences in the position and intensity of these bands suggest that the type of surfactant affects the local coordination environment and structural arrangement of the borate species during synthesis.

For the CTAB-assisted sample, distinct bands are observed at approximately 669, 975, 1058, 1267, and 1455 cm^{-1}. The strong bands around 975–1267 cm^{-1} are characteristic of B–O stretching vibrations in borate groups, while the band at approximately 669 cm^{-1} can be related to bending vibrations within the borate network. The relatively well-defined borate-related bands suggest a comparatively organized borate structure. In addition, the bands at approximately 2992 and 3560 cm^{-1} can be assigned to C–H stretching vibrations of residual organic species and O–H stretching vibrations of surface hydroxyl groups/adsorbed water, respectively.

In the SB12-supported nickel borate sample, bands are observed at approximately 680, 891, 1056, 1394, and 1557 cm^{-1}. The bands at 891 and 1056 cm^{-1} can be associated with B–O vibrations. The band around 680 cm^{-1} is associated with borate bending/lattice vibrations. Compared to CTAB, the bands at 1394 and 1557 cm^{-1} indicate differences in the local binding environment and/or surface species arising from the zwitterionic structure of SB12. The bands around 2900 and 2972 cm^{-1} belong to aliphatic C–H stretching vibrations. This suggests that small amounts of organic surfactants or carbon-containing species may remain on the sample surface. The weak band at 3661 cm^{-1} is consistent with O–H groups bound by weak hydrogen bonds. The SDS-assisted sample exhibits bands at approximately 573, 695, 892, 1051, 1249, and 1364 cm^{-1}. Bands around 892, 1051, 1249, and 1364 cm^{-1} are primarily associated with different B–O stretching modes. Bands at 573 and 695 cm^{-1} are associated with lower-frequency borate/lattice vibrations. The bands at 2897 and 2972 cm^{-1} can be attributed to aliphatic C–H stretching originating from SDS or organic species. A weak absorption band at 3675 cm^{-1} represents surface hydroxyl groups. Absorption bands in the 800–1400 cm^{-1} region support the formation of a borate-containing network [20].

The SDS sample shows additional banding at 573 and 1249 cm^{-1}, while the CTAB sample exhibits a distinct banding at 1267 cm^{-1}. In contrast, the SB12 sample exhibits characteristic bands at 891, 1394, and 1557 cm^{-1}. The C–H stretching bands around 2900–3000 cm^{-1} observed in all samples indicate the presence of residual surfactant-derived organic groups. The O–H related bands at approximately 3560–3675 cm^{-1} can be attributed to the presence of surface hydroxyl groups and/or adsorbed moisture. Overall, the FTIR results indicate that the type of surfactant affects the binding environment and surface chemistry of the synthesized nickel borate materials. The common B–O related bands show that the basic borate structure is preserved in all three samples. The FTIR results are also consistent with the expected surfactant-dependent morphological and crystalline structural differences observed by SEM and XRD.

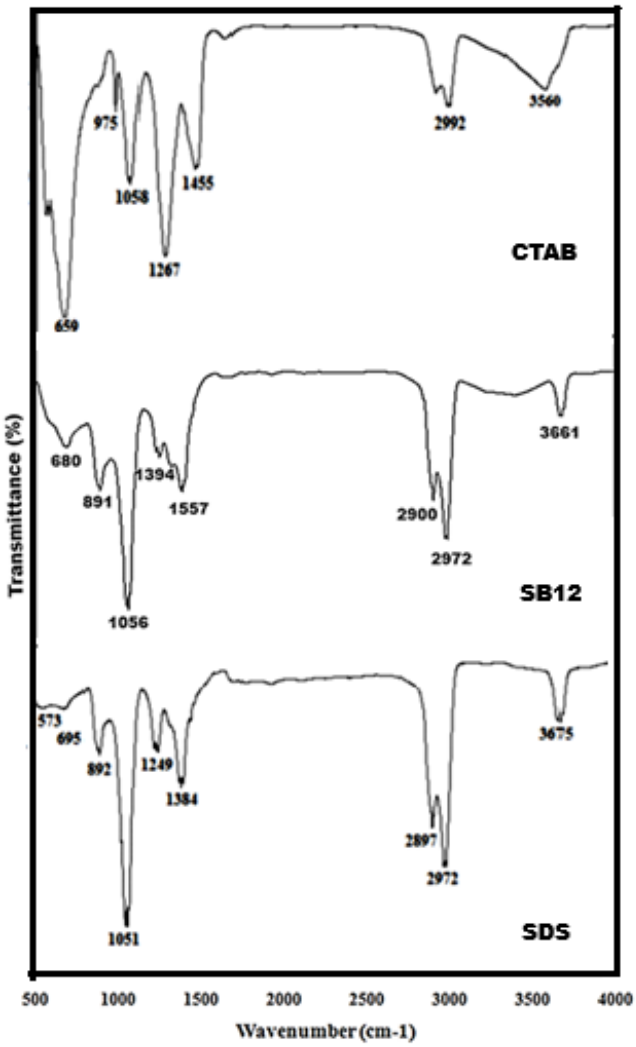

Figure 4. FTIR spectrum of nickel borate samples synthesized in CTA, SB12, and SDS surfactants

3.4. Thermal Analysis

The thermal behavior of synthesized nickel borate samples prepared by precipitation using CTAB, SB12, and SDS was investigated by simultaneous TG-DTA analysis, and the TG curves of the samples are given in Figure 5. TG curves show three characteristic mass loss regions. The first mass loss, observed below approximately 120 °C, indicates the removal of physically adsorbed water and residual solvent molecules. The second and most significant mass loss occurs between 120 and 300 °C. This mass loss is a result of the removal of chemically bound water, the dehydroxylation of amorphous nickel borate, and the thermal decomposition of CTAB, SB12, or SDS remaining among the post-synthesis nanoparticles.

As seen from the TG curves, a decrease in mass loss at temperatures above 300 °C demonstrates that many volatile species are removed and the borate skeleton becomes more stable. In samples synthesized with SDS surfactant, mass loss continues up to approximately 750 °C. This indicates the presence of a greater number of organic species in these synthesized samples. On the other hand, the fact that the least mass loss occurs in samples synthesized with CTAB surfactant indicates that it has better thermal stability. At 950 °C, the residual masses for CTAB, SB12, and SDS are 65-66%, 62-63%, and 56-57%, respectively, which shows that the thermal stability ranking is CTAB > SB12 > SDS.

The DTA curves of all three samples are shown in Figure 6, which illustrate the crystallization behavior of the amorphous material. As seen in Figure 6, the weak endothermic peak observed at temperatures between approximately 25-150 °C corresponds to the removal of adsorbed moisture. These results are consistent with TG mass loss. On the other hand, the most interesting case is the exothermic peak occurring between 650-750 °C. However, no significant mass loss is observed in the TG curves between these temperatures, indicating that this exothermic peak is due to crystallization rather than thermal decomposition.

According to the XRD results, it is seen that the initially formed amorphous structure transforms into a crystalline structure at temperatures above 700 C and the formation of thermodynamically stable orthorhombic nickel borate ($Ni_3(BO_3)_2$) takes place. DTA curves also support the XRD results. This situation appears as a characteristic feature for many amorphous inorganic substances prepared by wet chemical methods [21].

Therefore, the exothermic peak observed in the DTA curves confirms the crystallization temperature of amorphous nickel borate and supports the selection of 800 °C as the appropriate calcination temperature for obtaining crystalline $Ni_3(BO_3)_2$ in phase purity.

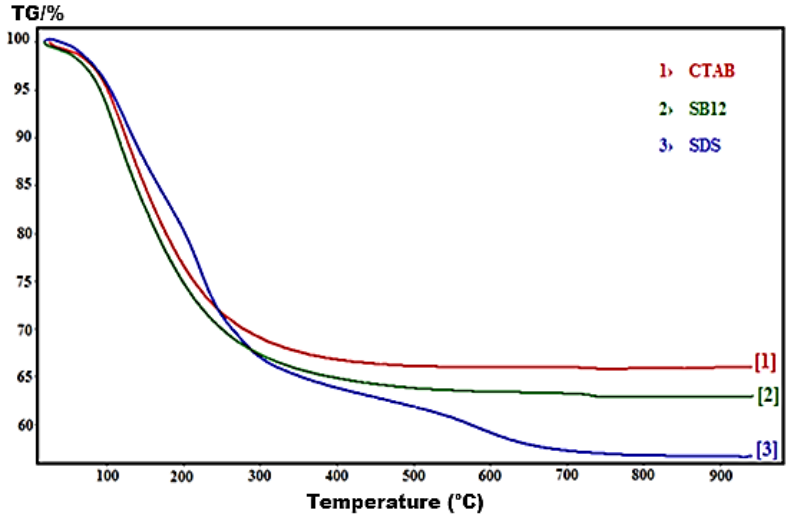

Figure 5. TG curves of nickel borate samples

4. Conclusion

In this study, orthorhombic nickel borate ($Ni_3(BO_3)_2$) was obtained by precipitation using CTAB, SB12, and SDS surfactants, followed by calcination at 800°C. Surfactant-assisted syntheses are being implemented as an effective strategy for producing nickel borate materials for advanced technological applications. Structural analysis confirmed the formation of the crystalline borate phase, while FTIR spectroscopy demonstrated the presence of borate functional groups. Morphological studies show the formation of porous, aggregated particles. Thermal analysis results reveal excellent thermal stability. Among the surfactants studied, CTAB provided the most homogeneous morphology and the highest thermal stability, while SB12 promoted crystal growth and SDS produced finer nanoparticles. These findings demonstrate that surfactant chemistry is an effective tool in shaping nickel borate microstructures and can be used in future catalytic and electrochemical applications.

Declaration of Conflict of Interests

The authors declare that there is no conflict of interest. They have no known competing financial interests or personal relationships that could have appeared to influence the work reported in this paper.

References

[1.] Ozer, D., Ozyavas, Z., Kaya, C., & Shiddique, S. Rapid and energy-efficient synthesis of nickel borate via solution combustion method for esterification reactions. Journal of Molecular Structure, 2025; 144815.

[2.] Qian, H., Sun, F., Zhang, W., Huang, C., Wang, Y., & Fang, K. Efficient metal borate catalysts for oxidative dehydrogenation of propane. Catalysis Science & Technology, 2022; 12(6); 1996-2005.

[3.] Mutailipu, M., Poeppelmeier, K. R., & Pan, S. Borates: A rich source for optical materials. Chemical Reviews, 2020; 121(3); 1130-1202.

[4.] Sun, X., Zhao, K., Liu, Z., Feng, Z., Wang, Z., Cui, L., & Liu, J. Facile electrodeposition of Ni3 (BO3) 2 nanospheres on Ti mesh for high-performance asymmetric supercapacitors. Journal of Energy Storage, 2022; 55; 105763.

[5.] Liu, X., Zhu, W., Cui, X., Liu, T., & Zhang, Q. Facile thermal conversion route synthesis, characterization, and optical properties of rod-like micron nickel borate. Powder technology, 2012; 222; 160-166.

[6.] Pang, H., Lu, Q., Chen, C., Liu, X., & Gao, F. Facile synthesis of Ni 3 (BO 3) 2 nanoribbons and their antimicrobial, electrochemical and electrical properties. Journal of Materials Chemistry, 2011; 21(36); 13889-13894.

[7.] Qin, W., Liu, Y., Liu, X., & Yang, G. Facile and scalable production of amorphous nickel borate for high performance hybrid supercapacitors. Journal of Materials Chemistry A, 2018; 6(40); 19689-19695.

[8.] Xu, B., Liu, Y., Tian, J., Ma, X., Ping, Q., Wang, B., & Xia, Y. Ni3 (BO3) 2 as anode material with high capacity and excellent rate performance for sodium-ion batteries. Chemical Engineering Journal, 2019; 363; 285-291.

[9.] Liang, P., Du, L., Wang, X., & Liu, Z. H. Preparation of Ni3B2O6 nanosheet-based flowerlike architecture by a precursor method and its electrochemical properties in lithium-ion battery. Solid state sciences, 2014; 37; 131-135.

[10.] Ai-Min, C., Feng-Chao, H., Pei, G., & Zhe-Ming, N. Sol-gel synthesis, characterization of nickel borate nanorods. Chinese Journal of Inorganic Chemistry, 2011; 27; 30-34.

[11.] Cao, J., Wang, Y., Song, X., & Feng, J. One-dimensional nickel borate nanowhiskers: characterization, properties, and a novel application in materials bonding. RSC advances, 2014; 4(37); 19221-19225.

[12.] Menezes, J. C. A., Ferreira, N. S., Abraçado, L. G., & Macêdo, M. A. Synthesis and characterization of nickel nanoparticles prepared using the aquolif approach. Journal of Nanoscience and Nanotechnology, 2014; 14(8); 5903-5910.

[13.] Raza, W., & Umar, K. Cost-effective non-precious nickel borate nanorods for integrated energy and environmental applications. International Journal of Hydrogen Energy, 2026; 219; 154079.

[14.] Somanath, B. C. M., Athreya, Y., Shwetha, K.P., Abraham, N., Viswanathan, S. B., & Khosla, A. Scalable synthesis of $Ni_3B_2O_6$ nanograins and fabrication of a coin cell supercapacitor for powering temperature sensor devices. ACS Applied Electronic Materials, 2023; 5(9); 5005-5016.

[15.] Lofland, S. E., Ramanujachary, K. V., & Ganguli, A. K. A new low temperature methodology to obtain pure nanocrystalline nickel borate. Journal of Organometallic Chemistry, 2010; 695(7); 1002-1005.

[16.] Samiey, B., Cheng, C. H., & Wu, J. Effects of surfactants on the rate of chemical reactions. Journal of chemistry, 2014; 1; 908476.

[17.] Bakshi, M. S. How surfactants control crystal growth of nanomaterials. Crystal Growth & Design, 2016; 16(2); 1104-1133.

[18.] Sharma, S., Ramanujachary, K. V., Lofland, S. E., & Ganguli, A. K. Controlling the size and morphology of anisotropic nanostructures of nickel borate using microemulsions and their magnetic properties. Journal of colloid and interface science, 2011; 360(2); 393-397.

[19.] Ghosh, S., Ray, A., Pramanik, N. Self-assembly of surfactants: An overview on general aspects of amphiphiles. Biophysical Chemistry, 2020; 265; 106429.

[20.] Türk, M., Gümüş, B., Ustun, F., & Balköse, D. Nano-sized nickel borate preparation and characterization. In High-Performance Materials and Engineered Chemistry 2018; (pp. 313-336). Apple Academic Press.

[21.] Ozer, D., Ozyavas, Z., Kaya, C., & Shiddique, S. (2025). Rapid and energy-efficient synthesis of nickel borate via solution combustion method for esterification reactions. Journal of Molecular Structure, 144815.

How to Cite This Article

Güner, E.K, and Özer, A. K., Effect of Surfactants on The Structural, Morphological and Thermal Properties of Nickel Borate Synthesized by Co-Precipitation, Brilliant Engineering, 4(2026), 41165.
https://doi.org/10.36937/ben.2026.41165